

Specific RCS for Describing the Scattering Characteristic of Complex Shape Objects

Mariya S. Antyufeyeva¹, Alexander Yu. Butrym¹, Nikolay N. Kolchigin¹, Maxim N. Legenkiy¹, Alexander A. Maslovskiy^{1, *}, and Gennady G. Osinovy²

Abstract—Nowadays it is important to create military and civilian vehicles which would be invisible to radar (or homing precision weapons). Such a task requires using high amount of radio-absorbing materials and high cost of finished samples of re-engineering. So it is very useful to have some methods for mathematical modeling of electromagnetic waves scattering on the object in order to take into account various techniques to reduce the object visibility at the stage of design. After the mathematical modeling for each case (specified wavelength, polarization, background surface, etc.), we obtain the angular RCS dependence. We obtain such dependencies for two different models. Based on the comparison of these two dependencies for different objects, it is very difficult to determine which one of the objects is more detectable. This paper presents a new calculation method which allows characterizing the scattering properties of each object only with a few numbers: specific RCS (same as normalized RCS) and RCS dispersion. The presented method can be simply used to assess the visibility of the objects placed on different background surfaces.

1. INTRODUCTION

Radar cross section (RCS) controlling is useful for aeronautics and defense industry in order to obtain important information about an object before it is built. For many industries (for example military), some detectability reducing methods are required. For this purpose, one can use object cloaking with RAM (Radio Absorbing Materials) [1, 2] or some object shape changing [3]. RCS prediction saves time and resources. For these aims, investigators should propose some efficient techniques. One of the ways for RCS prediction is RCS measurements. However, these measurements suffer from several technical complexities and have high cost [4].

Analytical calculation methods cannot be used for RCS calculation of the complex shape objects, so in this case some numerical approaches should be treated [5]. For example, one can apply facet method [6, 7] or the approach of Sukharevsky [8]. There are also methods which allow the RCS calculation for multilayer structures of dielectric and magnetic materials [9]. However, these techniques can be computationally hard even for modern supercomputers or suffer from several mistakes in the case when the surface has a lot of small details and parts with significant inverse scattering due to re-reflections.

One of the most effective RCS calculation techniques is Physical Optics — Shooting and Bouncing Ray (PO-SBR) method [10], which is now adopted for the calculations between the object's parts [11, 12], and for receiving some additional information about the target [13]. In [14] and [15], some variations of PO-SBR method for fast computation of the complex shape radiolocation targets are considered. In this paper, for RCS calculations we use a 3D program similar to [16] programs based on PO-SBR method.

Received 29 April 2016, Accepted 21 October 2016, Scheduled 13 December 2016

* Corresponding author: Alexander A. Maslovskiy (alex.maslovesky@gmail.com).

¹ Karazin Kharkiv National University, 4, Svobody sq., Kharkiv 61022, Ukraine. ² Yuzhnoye State Design Office, 3, Krivorozhskaya st., Dnepropetrovsk 49008, Ukraine.

When evaluating the radar visibility of ground object, reflection from the surface must be taken into account [3, 17]. In such calculations, it is necessary to consider roughness of the surface and electromagnetic properties [18, 19]. There are a lot of works about scattering properties of different background surfaces [20] and on-ground objects (see [21, 22]). Effective calculation algorithm for obtaining on-ground object RCS was proposed in [21], see using example in [8]. However, technique mentioned above supposes re-calculation for each new background surface (with other electromagnetic characteristics). In order to circumvent this difficulty, the following method was proposed by authors in [23]. In this case, the full scattered field for on-ground object is presented in the form of series over powers of background surface reflection coefficient.

With the help of this calculation method, one can obtain the RCS angular dependence — Backscatter Pattern (BSP). In real situations, radar can see the target from different observation angles, and RCS has some random values [24]. These random values are simply used to obtain RCS probability distribution — probability to obtain some RCS value [25]. Further for the detection probability calculation, this distribution can be approximated by some known Probability Distribution Functions (PDF). For example, in [26] the authors use χ^2 and lognormal PDFs for the RCS distribution approximation for some stealth targets. In [27], the distribution in the form of sum of Gaussian distribution is treated for this purpose.

However, using the PDF approximation by some known distributions can give some errors, which are significant when calculated BSP contains large peaks for narrow angular ranges — “highlights”. Sometimes before the PDF approximation, some data averaging is provided [24]. This eliminates the “highlights” contribution but can give some errors in calculations.

In this paper for the PDF approximation, we use the sum of delta functions as proposed by the authors in [23]. This allows us to avoid the drawback mentioned above and to obtain the formula for detection probability calculation in closed form.

The described approach for detection probability calculation has another disadvantage: we need to provide new calculations for each separate radar with some new characteristics. In order to avoid this problem, in this paper we propose to describe the complex shape radar target by a few numbers: specific RCS and RCS dispersion. This allows us to simply recalculate the detection probability of the objects placed on different background surfaces for the radars with different parameters.

So in the first section of the paper, we describe the method of RCS calculation for arbitrary background surface. In the second section, the method of detection probability defining will be presented. In the third section, formula obtained for detection probability calculation will be analyzed, and specific RCS will be introduced.

2. RCS CALCULATION

In this paper, as input data we consider the BSP obtained at wavelength 3 cm for horizontal polarization for two models of truck KRAZ. In order to show radar detectability reduction, we consider two KRAZ models with and without cloaking (Fig. 1). Both models were created with the help of 3D designer program.

For following estimation of the object detectability, it is necessary to calculate its backscattering pattern (BSP) when being placed on different types of background surface. In order to calculate the scattered field for the objects situated on different background surfaces, we use the technique proposed in [23]. In our considerations, the background surface is characterized by two parameters:

- Backscattering reflection which is conditioned by diffusive scattering at the surface irregularities. It creates “background” scattering signal, on which the object is to be detected. This parameter is not involved in calculation of the object’s BSP; it is taken into account below in statistical data processing.
- Specular reflection that influences the backscattering from the object due to rays that bounce between the object and the background surface.

Here we divide these two types of reflections and consider them as independent.

The former parameter is described with specific RCS of the surface backscattering σ_{spec} [28], and it is described by some probability density function.

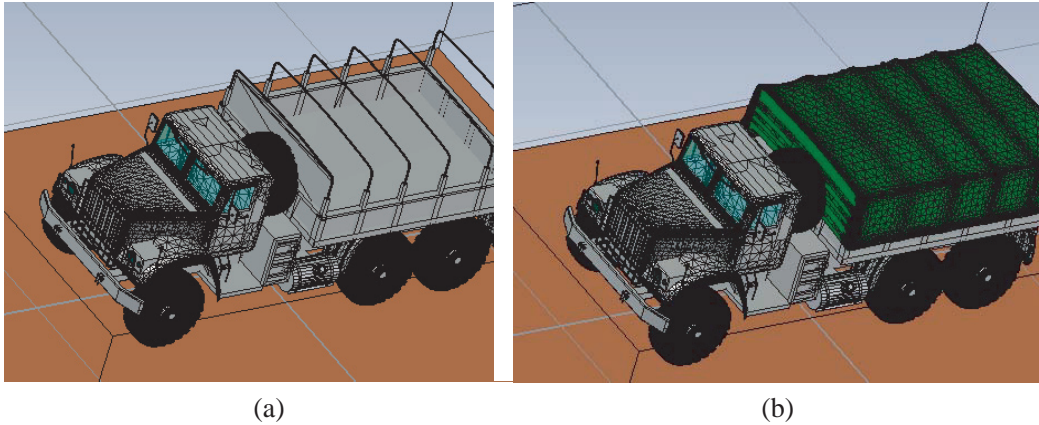


Figure 1. KRAZ models. (a) Model 1 — Source KRAZ model. (b) Model 2 — KRAZ model with cloaking.

Typically, calculation of the object BSP takes the most time (99% of the total detectability estimation time), at which for any required background surface type it requires separate long calculations. In order to optimize this process and to be able to analyze BSP for a wide range of possible background surfaces, the authors propose the calculation scheme based on decomposing the reflected field [29]. Thus, the scattered field can be divided into the following components:

1. The rays that are incident onto the object and reflected backwards;
2. The rays that are incident onto the object, then reflected towards the background surface and finally reflected towards the radar;
3. The rays that are incident onto the background surface, then reflected towards the object and finally reflected towards the radar;
4. The rays that are incident onto the background surface, then reflected towards the object, then reflected back to the background surface, and finally reflected towards the radar.

The reflected field E_0 (see Fig. 3) created by the rays from case 1 does not interact with the background surface and thus, does not depend on the surface reflection coefficient (R). The reflected field E_1 created by the rays from cases 2 and 3 interacts with the background surface only once, and hence it is proportional to R . Finally, the field component E_2 is created by rays 4, and it interacts with the background surface twice, hence is proportional to the squared reflection coefficient R^2 . Fig. 3 schematically illustrates the above described interaction cases.

Thus, neglecting the further multiple reflections between the object and the ground, we can assume that the reflected field depends on the background surface reflectance R by the following law:

$$E(R) = E_0 + R \cdot E_1 + R^2 \cdot E_2 \quad (1)$$

Since the background surface is assumed to be infinite plane. The reflected field will be contributed only by the rays bouncing off the surface at the incidence angles that correspond to the radar elevation position. Hence in the case that R is dependent on the incidence angle (e.g., by Fresnel formulae), the equation contains R for the given incidence angle θ .

Then we should perform simulation of the electromagnetic wave diffraction on radar target for the three cases:

1. The object is placed in a free space without any background surface, and the result is a complex value of the scattered field E_{AIR} .
2. The object is over a perfectly electrically conducting (PEC) surface (the surface impedance is zero, and the reflectance is $R = -1$), and the result is a complex value of the scattered field E_{PEC} .
3. The object is over a perfectly magnetically conducting (PMC) surface (the surface impedance is infinite, and the reflectance is $R = 1$), and the result is a complex value of the scattered field E_{PMC} .

From such modeling, all three scattered field components can be derived in correspondence with formula (1):

$$\begin{aligned} E_0 &= E_{AIR}, \\ E_1 &= 0.5 (E_{PMC} - E_{PEC}), \\ E_2 &= 0.5 (E_{PMC} + E_{PEC}) - E_{AIR}. \end{aligned} \quad (2)$$

Thus, after these three simulations, we obtain the results that allow us to find BSP for any other background surface with known reflection coefficient R .

Numerical experiments with the help of formulae described above allow showing that for some vehicle situated on background surface, the significant part of reflected field is conditioned by re-reflections between sidewalls of the object and background surface (they form some “corner reflector” [30]). It is pointed out that using inclined sidewalls of radar targets can reduce the component of the scattered field discussed above [3].

3. DETECTION PROBABILITY CALCULATION

As a calculation result, we have RCS of the object on a specific background surface as a function of azimuth angle $\sigma_i = \sigma(\varphi_i)$.

In Fig. 2, the dependencies for concrete background surface (lossless dielectric with permittivity $\varepsilon = 5.5$) are presented.

The radar can see object from different unpredictable directions. So, the RCS of the target is a random signal, and possibility to detect or not to detect the target can be considered from the statistical point of view. The content of this paragraph was briefly described in our conference paper [23], and now we present the extended version of this paper with some new results.

For our case, the obtained RCS angular dependencies have statistical parameters presented in Table 1.

It is important to mention that the mean and median values from Table 1 seem very large. That is why in our calculations we take into account the specular reflection from near-object part of the substrate. Another reason for the big values in Table 1 is the presence of some “corner reflectors” in the investigated model [3, 30].

For obtained data, we can draw histograms (see Fig. 4) where the solid bars designate data for model 1 and the empty bar for model 2. Here in x -axis, one can see the RCS values in logarithmic scale, in y -axis — the probability to obtain corresponding RCS value. Histograms in Fig. 4 are plotted with 50 pins.

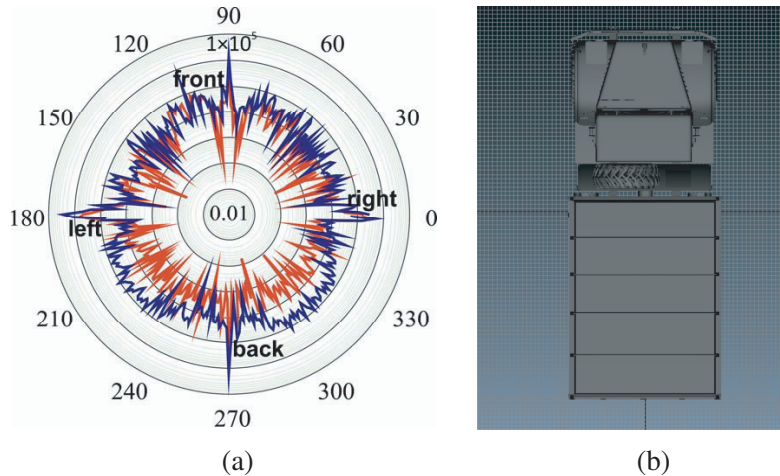


Figure 2. Angular dependence of RCS in m^2 for Model 1 (solid line) and Model 2 (dotted line) and (b) KRAZ position.

Table 1. RCS data in m^2 from Fig. 2.

Parameter	Model 1	Model 2
minimum	4.668	0.551
maximum	2.782×10^4	6.365×10^3
mean value	538.216	188.182
median value	228.749	62.156

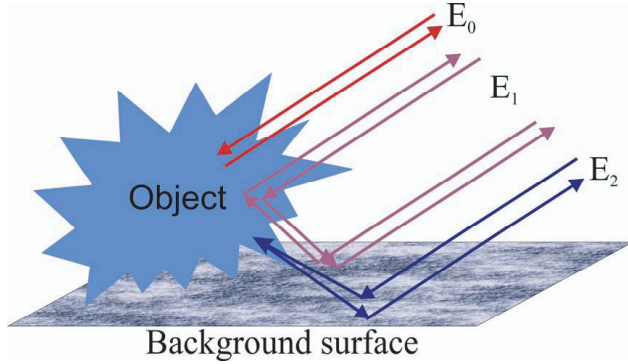


Figure 3. Object on background surface.

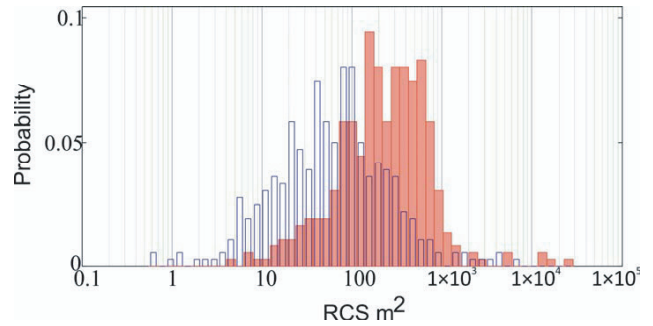


Figure 4. Histograms for data in Fig. 2 (red filled columns — RCS of model 1, empty columns — RCS of model 2).

Of course, obtained RCS data can be approximated by some PDFs [24] for simplifying the following calculations. However, this can give significant errors in the case that BSP has many sharp highlights corresponding to specular reflections from different parts of the object. So, we can consider the obtained data without any approximations as a sum of delta functions which have peaks in the points corresponding to the calculated RCS values σ_i and have amplitudes $1/N$ (the probability to obtain RCS value σ_i) [23]:

$$F_{obj}(u) = \sum_{i=1}^N \delta(u - \sigma_i) / N \tag{3}$$

In all discussions above we do not take into account the diffuse scattering from background surface. This is a rough surface, so its RCS can be considered as a random signal [31]. In our calculations, we suppose that this random signal satisfies Rayleigh PDF

$$F_{bg}(u, s) = (u/s^2) \exp(-u^2/2s^2) \tag{4}$$

Here u is the random RCS value and s the distribution parameter that corresponds to the median of the random value. In our calculations, we consider concrete as a rough surface. For the case under study (wavelength, incident angle), the specific RCS is equal to $\sigma_{sp} = -46.7 \text{ dBm}^2$ [20].

In the case that the radar lights the part of background surface with area S_L , we obtain the distribution parameter s in distribution of Eq. (4) for the given background surface as

$$s = \sigma_{sp} S_L. \tag{5}$$

The illuminated part of background surface S_L is determined by some parameters of radar station (distance to the station, beam width of radiation pattern).

Now we should take into account the probability distribution for the considered object and the diffuse scattering from background. So, we should add two random signals: calculated RCS for object in Eq. (3) and RCS for background surface in Eq. (4). Here we consider these signals as independent ones, and as a result, we obtain the convolution of the distributions in Eqs. (3) and (4), which can be

calculated in a closed form as a sum of functions in Eq. (4) with offset arguments $u - \sigma_i$:

$$F_{obj+bg}(u, s) = \int_0^\infty F_{obj}(\nu)F_{bg}(u - \nu, s)d\nu = \sum_{i=1}^N F_{bg}(u - \sigma_i, s)/N \quad (6)$$

Now we obtain the full distributions for investigated objects as a sum of offset Rayleigh distributions.

Histograms (for the case of 50 pins) for two considered objects are shown in Fig. 5. The solid jagged lines here are the full object RCS distributions obtained with the help of formula (6) in the case that Rayleigh distribution parameter is equal to $s = 20$. For model 1, this line is a good approximation of calculated histogram — this object is well visible on the background surface. For model 2, this line is more corrupted in comparison with histogram — the object is not so well visible as the first one.

From obtained RCS probability distributions, we can estimate the detection probability for the given radar resolution (dr — the side of the square that is lighted by the radar beam on background surface). For this aim, we should define some threshold RCS σ_{th} . Usually σ_{th} is chosen from conditions that false alarm probability is equal to value P_{fa} (often and in this work below $P_{fa} = 10^{-4}$). False alarm probability P_{fa} is a probability that radar detects background. So, we have the following relation to obtain σ_{th}

$$P_{fa} = \int_{\sigma_{th}}^\infty F_{bg}(u, s)du = 1 - \int_0^{\sigma_{th}} F_{bg}(u, s)du \quad (7)$$

Equation (7) leads to $\sigma_{th} = (-\ln(P_{fa})2s^2)^{1/2}$.

Now we can calculate the detection probability for the given radar resolution

$$P_{det} = \int_{\sigma_{th}}^\infty F_{obj+bg}(u, s)du = 1 - \sum_{i=1}^N \int_0^{\sigma_{th}} F_{bg}(u - \sigma_i, s)du/N \quad (8)$$

For the case that the background surface PDF has the form in Eq. (4), and the integrals in Eq. (8) can also be calculated in closed form and expressed in form

$$P_{det} = 1 - \sum_{i=1}^N \left(1 - \exp\left(-\frac{(\sigma_{th} - \sigma_i)^2}{2s^2}\right)\right) / N = \frac{1}{N} \sum_{i=1}^N \exp\left(-\frac{(\sigma_{th} - \sigma_i)^2}{2s^2}\right) \quad (9)$$

However, formula (9) needs some corrections. For calculations of σ_{th} , we need the area of the illuminated part of the background surface (see formula (5)). However, the investigated object shades some part of this surface. We designate this shaded part of the surface for each direction (with RCS σ_i) as S_i^{sh} . So, in P_{det} calculations for each direction (with RCS σ_i), we should use $S_L - S_i^{sh}$ instead of S_L . Using formula (5), we obtain the following expression for P_{det} calculation

$$P_{det} = \frac{1}{N} \sum_{i=1}^N \exp\left(-\frac{(\sigma_{th} - \sigma_i)^2}{2\sigma_{sp}^2 (S_L - S_i^{sh})^2}\right) \quad (10)$$

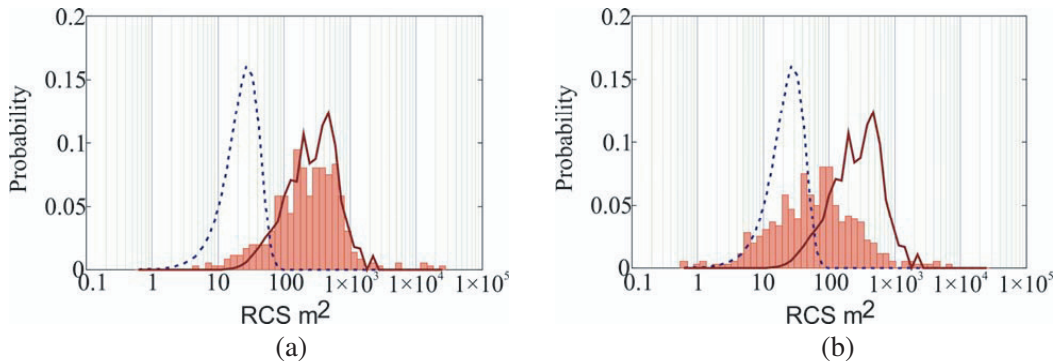


Figure 5. Full RCS probability distributions for different models (solid jagged lines — full object RCS distributions obtained with the help of formula (6) in the case when Rayleigh distribution parameter $s = 20$, dashed line- distribution for background surface). (a) For model 1. (b) For model 2.

For a certain direction, the visible area of the object can be larger than the illuminated part of the background surface $S_i^{sh} > S_L$ — for this direction, the radar sees only the object. In this case, if the RCS for lighted object part for this direction σ_i is larger than σ_{th} , we add to the detection probability a value $1/N$. Using these considerations, we can write the final formulae for detection probability calculation in the following form

$$P_{det} = \frac{1}{N} \sum_{i=1}^N \begin{cases} \exp\left(-\frac{(\sigma_{th} - \sigma_i)^2}{2\sigma_{sp}^2 (S_L - S_i^{sh})^2}\right), & S_i^{sh} < S_L; \\ \eta(\sigma_i - \sigma_{th}), & S_i^{sh} > S_L; \end{cases} \quad (11)$$

Here $\eta(x)$ is Heaviside function (unit step function): $\eta(x) = 1$ for $x > 0$ and $\eta(x) = 0$ for $x < 0$.

As a result of calculation by formula (11), one obtains the detection probability for the object on the given background $0 < P_{det} < 1$.

The above mentioned shadowed area S_i^{sh} is calculated in the assumption of parallelepiped shape of the object. Under any angle of view, three walls of the parallelepiped are seen. Suppose that we know height h , length l and width w of the parallelepiped. Then, if it is illuminated by a source from the i -th direction with angle coordinates θ_i from zenith and azimuth φ_i from the direction along the length, the area of the shadow can be calculated with the following formula:

$$S_i^{sh}(\theta_i, \varphi_i) = h \cdot \tan \theta_i \cdot (l \cdot |\cos \varphi_i| + w \cdot |\sin \varphi_i|) + w \cdot l \quad (12)$$

For example, Fig. 6 shows the dependence of the shadowed area on the azimuth angle for the object under consideration (model 1) at incidence angle $\theta = 40^\circ$ from zenith. After cloaking (for model 2), the dimensions of the object are not changed significantly.

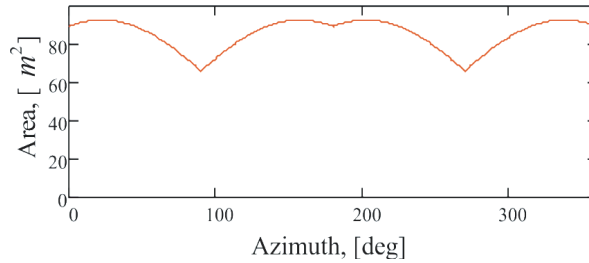


Figure 6. The shadowing area for the object under consideration (height $h = 4.372$ m, length $l = 10.937$ m and width $w = 4.559$ m).

4. DETECTION PROBABILITY ANALYSIS

In fact, the detection probability for any specific object is a function of the lighted area of background surface S_L and of the background specific RCS σ_{sp} . The lighted area of background surface S_L is defined by the radar antenna pattern, and further we consider this area as square with side dr (radar resolution), then $S_L = dr^2$.

The following dependence of detection probability on radar resolution (detection curves) for the background specific RCS $\sigma_{sp} = 5.926$ was obtained by technique described above.

Here one can see that for small radar resolutions, the detection probability is equal to $P_{det} = 1$ — the object will be detected, and for big radar resolution the detection probability is equal to $P_{det} = 0$ — the object is not visible on the background surface.

The crossing points of the 0.5 level are marked on the plot, and they correspond to radar resolution required for object detection with 50% probability. In this case, applying cloaking has led to reducing (improving) required resolution by factor $P_{0.5}/P'_{0.5} = 1.955$ or by 5.824 dB (see Fig. 7). Of course, $P_{0.5}$ can be taken as a numerical value of the cloaking effectiveness. However, this value should be recalculated for another background surface (sand, grass or forest).

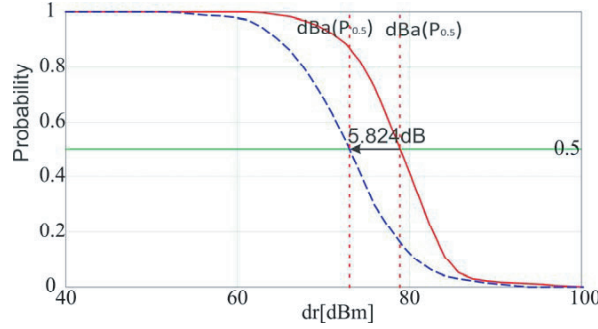


Figure 7. Dependence of detection probability on radar resolution for model 1 (solid line) and model 2 (hatch line).

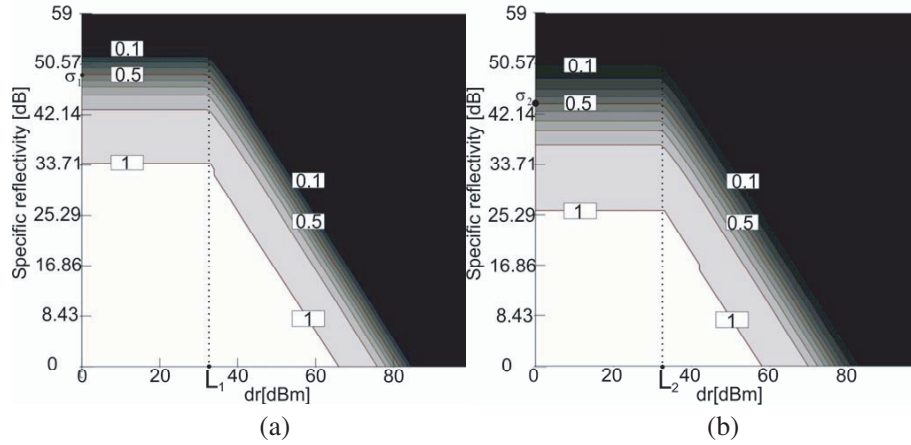


Figure 8. Dependence of P_{det} on background specific RCS and on radar resolution for the (a) model 1 and (b) model 2. White color — $P_{det} = 1$, black — $P_{det} = 0$.

In order to understand how the detection probability P_{det} behaves when varying both radar resolution and background level let’s plot two parametric dependences. In Fig. 8, the plot of such dependence is given in the form of level lines. From the plot one can see that when the radar resolution is below the object size (i.e., when the low part of formula (11) works), the detection probability does not depend on the resolution and remains constant. In the case of large resolution when background specific RCS is decreased by x dB and the radar resolution increased by x dB, then the detection probability remains the same.

So, the 0.5 level lines in the figure can be characterized by two numbers: “background specific RCS” that under small radar resolution provides 0.5 detection probability, and “effective object size”, at which the transition from the constant regime to the linear dependence regime occurs. The former parameter can be called “object specific RCS” (in Fig. 8. $\sigma_1 = 48.85$ [dB] and $\sigma_2 = 43.77$ [dB]), and the latter — “object visible area” (in Fig. 8. $L_1 = L_2 = 33.74$ [dBm]).

These parameters can be defined when we consider formula (11) as a function of two variables: object specific RCS σ_{sp} and radar resolution dr ($S_L = dr^2$) — $P_{det} = P_{det}(\sigma_{sp}, dr)$. The object specific RCS can be defined as the maximum σ_{sp} which the equation $P_{det}(\sigma_{sp}, 0) = 1$ satisfies for.

For example, for the considered objects in this paper, we have specific RCS $\sigma_1 = 48.85$ [dB] for model 1 and $\sigma_2 = 43.77$ [dB] for model 2.

Figure 8 shows the dependencies for the object before and after cloaking. So, one can see that after cloaking the level lines along axis y decrease by constant value for all radar resolutions. Also on the linear part of the plot (when RCS is small), it can be interpreted as shift to the left by the same value (in dB). This shift can be used as a numerical value of effectiveness of the object detectability reducing. So for the considered case, cloaking effectiveness can be “measured” as $\Delta\sigma = \sigma_1 - \sigma_2 = 5.08$ [dB].

5. CONCLUSIONS

In this paper, we propose a methodology for calculating object detectability. For this purpose, we should estimate specific RCS of the object with the help of obtained formulae. This concept allows us to abstract from providing any specific background signal level and radar station parameters. From obtained values, we can calculate the object detection probability in the case of arbitrary background level and arbitrary radar resolution.

It should be noticed that the object specific RCS can be directly compared to the background specific RCS in order to make an immediate conclusion regarding detectability of the object on such a background when a sufficiently good radar is used (that have resolution smaller than the object size).

REFERENCES

1. Taravati, S. and A. Abdolali, "A new three-dimensional conical ground-plane cloak with homogeneous materials," *Progress In Electromagnetics Research M*, Vol. 19, 91–104, 2011.
2. Wu, T. K., "From cloaking of conducting cylinder to RCS reduction/enhancement," *Radio Science Meeting (Joint with AP-S Symposium), USNC-URSI*, 133, IEEE, 2013.
3. Maslovskiy, A. and M. Legenkiy, "Geometrical techniques for reducing radar targets detectability," *Proceedings of Conference on Radiophysics, Electronics and Biophysics YSC*, Kharkiv, 2014.
4. Bouzidi, A. and T. Aguilu, "RCS prediction from planar near-field measurements," *Progress In Electromagnetics Research M*, Vol. 22, 41–55, 2012.
5. Baussard, A., M. Rochdi, and A. Khenchaf, "PO/mec-based scattering model for complex objects on a sea surface," *Progress In Electromagnetics Research*, Vol. 111, 229–251, 2011.
6. Borzov, A., A. Sokolov, and V. Suchkov, "Digital simulation of input signals of systems of a near radar-location from complex radar-tracking scenes," *Radio Electronics Magazine*, 2004 (in Russian).
7. Youssef, N., "Radar cross section of complex targets," *Proceedings of the IEEE*, Vol. 77, 722–734, May 1989.
8. Sukharevsky, O. I., *Electromagnetic Wave Scattering by Aerial and Ground Radar Objects*, 288, Taylor & Francis Group, CRC Press, 2015.
9. De Adana, F. S., I. Gonzalez, O. Gutierrez, and M. F. Catedra, "Asymptotic method for analysis of RCS of arbitrary targets composed by dielectric and/or magnetic materials," *IEEE Proceedings — Radar, Sonar and Navigation*, Vol. 150, No. 5, 375–378, 2003.
10. Ling, H., R.-C. Chou, and S.-W. Lee, "Shooting and bouncing rays: Calculating the RCS of an arbitrarily shaped cavity," *IEEE Trans. Antennas Propagat.*, Vol. 37, No. 2, 194–205, 1989.
11. Boag, E. M., "A fast physical optics (FPO) algorithm for double-bounce scattering," *IEEE Trans. Antennas Propagat.*, Vol. 52, 205–212, 2004.
12. Boag, A., "A fast physical optics (FPO) algorithm for high frequency scattering," *IEEE Trans. Antennas Propagat.*, Vol. 52, 197–204, 2004.
13. Bhalla, R., H. Ling, J. Moore, D. J. Andersh, S. W. Lee, and J. Hughes, "3D scattering center representation of complex targets using the shooting and bouncing ray technique: A review," *IEEE Antennas Propagat. Mag.*, Vol. 40, 30–39, 1998.
14. Tao, Y. B., H. Lin, and H. J. Bao, "Kd-tree based fast ray tracing for RCS prediction," *Progress In Electromagnetics Research*, Vol. 81, 329–341, 2008.
15. Gao, P. C., Y. B. Tao, Z. H. Bai, and H. Lin, "Mapping the sbr and tw-ildcs to heterogeneous cpu-gpu architecture for fast computation of electromagnetic scattering," *Progress In Electromagnetics Research*, Vol. 122, 137–154, 2012.
16. Rius, M., M. Ferrando, and L. Jofre, "GRECO: Graphical electromagnetic computing for RCS prediction in real time," *IEEE Antennas Propagat. Mag.*, Vol. 35, 7–17, 1993.
17. Man, M., Z. Lei, Y. Xie, and X. Li, "Bistatic RCS prediction of composite scattering from electrically very large ship-sea geometry with a hybrid facet-based ka and shadow-corrected greco scheme," *Progress In Electromagnetics Research B*, Vol. 60, 35–48, 2014.

18. Cocheril, Y. and R. Vauzelle, "A new ray-tracing based wave propagation model including rough surfaces scattering," *Progress In Electromagnetics Research*, Vol. 75, 357–381, 2007.
19. Du, Y. and B. Liu, "A numerical method for electromagnetic scattering from dielectric rough surfaces based on the stochastic second degree method," *Progress In Electromagnetics Research*, Vol. 97, 327–342, 2009.
20. Kulemin, G. P. and E. V. Tarnavskiy, "Modeling of interference map from ground surface for MMR radar stations for small angles sliding," *Radioelectronic and Computer Systems*, No. 1, 5–12, 2004.
21. Kovalev, S., S. Nesterov, and I. Skorodumov, "Determination RCS of objects with a glance of reflection from earth surface," *Radiotechniques and Electronics*, Vol. 41, No. 11, 1304–1310, 1996 (in Russian).
22. Akinshin, R., A. Khudyakov, V. Rumyantsev, and S. Kurbatsky "Evaluating the effectiveness of algorithms polarization selection stationary ground objects," *Radio Electronics Magazine* Vol. 4, 2013 (in Russian).
23. Legenkiy, M., A. Butrym, and M. Antyufeyeva, "Evaluation of on-ground object radar detectability reduction," *Proceedings of the Conference Mathematical Methods in Electromagnetic Theory*, 254–257, Dnipropetrovsk, Aug. 26–28, 2014.
24. Swerling, P., "Probability of detection for fluctuating targets," *IRE Transactions on Information Theory*, Vol. 6, No. 2, 269–308, 1960.
25. Bergamaschi, L., G. D'Agostino, L. Giordani, G. Mana, M. Oddone, "The detection of signals buried in noise," *Data Analysis, Statistics and Probability*, 1–12, 2013.
26. Shi, W., X.-W. Shi, and L. Xu, "RCS characterization of stealth target using χ^2 distribution and lognormal distribution," *Progress In Electromagnetics Research M*, Vol. 27, 1–10, 2012.
27. Zhuang, Y.-Q., C.-X Zhang, and X.-K. Zhang, "Accurate statistical modeling method for dynamic RCS," *PIERS Proceedings*, 1135–1139, Guangzhou, Aug. 25–28, 2014.
28. Corbel, C., C. Bourlier, N. Pinel, and J. Chauveau, "Rough surface RCS measurements and simulations using the physical optics approximation," *IEEE Trans. Antennas Propagat.*, Vol. 61, No. 10, 5155–5165, Oct. 2013.
29. Maslovskiy, A. A. and M. N. Legenkiy, "Analysis of geometrical techniques for reducing radar detectability of on-ground targets," *Proceedings of the International Young Scientist Forum on Applied Physics, (YSF'2015)*, 1–4, Dnipropetrovsk, Sep. 29–Oct. 1, 2015.
30. Kobak, V., "Radar reflectors," *Soviet radio*, 248, Moscow, 1975 (in Russian).
31. Wang, X., C.-F. Wang, Y.-B. Gan, and L.-W. Li, "Electromagnetic scattering from a circular target above or below rough surface," *Progress In Electromagnetics Research*, Vol. 40, 207–227, 2003.